HEPATOLOGY
Official Journal of the American Association for the Study of Liver Diseases

Differential Effects of Sorafenib on Liver Versus Tumor Fibrosis Mediated by Stromal-Derived Factor 1 Alpha/C-X-C Receptor Type 4 Axis and Myeloid Differentiation Antigen–Positive Myeloid Cell Infiltration in Mice

Yunching Chen,[1] Yuhui Huang,[1] Thomas Reiberger,[1] Annique M. Duyverman,[1] Peigen Huang,[1] Rekha Samuel,[1] Lotte Hiddingh,[1] Sylvie Roberge,[1] Christina Koppel,[1] Gregory Y. Lauwers,[2] Andrew X. Zhu,[3] Rakesh K. Jain,[1] and Dan G. Duda[1]

Sorafenib—a broad kinase inhibitor—is a standard therapy for advanced hepatocellular carcinoma (HCC) and has been shown to exert antifibrotic effects in liver cirrhosis, a precursor of HCC. However, the effects of sorafenib on tumor desmoplasia—and its consequences on treatment resistance—remain unknown. We demonstrate that sorafenib has differential effects on tumor fibrosis versus liver fibrosis in orthotopic models of HCC in mice. Sorafenib intensifies tumor hypoxia, which increases stromal-derived factor 1 alpha (SDF-1α) expression in cancer and stromal cells and, subsequently, myeloid differentiation antigen–positive (Gr-1$^+$) myeloid cell infiltration. The SDF-1α/C-X-C receptor type 4 (CXCR4) pathway directly promotes hepatic stellate cell (HSC) differentiation and activation through the mitogen-activated protein kinase pathway. This is consistent with the association between SDF-1α expression with fibrotic septa in cirrhotic liver tissues as well as with desmoplastic regions of human HCC samples. We demonstrate that after treatment with sorafenib, SDF-1α increased the survival of HSCs and their alpha-smooth muscle actin and collagen I expression, thus increasing tumor fibrosis. Finally, we show that Gr-1$^+$ myeloid cells mediate HSC differentiation and activation in a paracrine manner. CXCR4 inhibition, using AMD3100 in combination with sorafenib treatment, prevents the increase in tumor fibrosis—despite persistently elevated hypoxia—in part by reducing Gr-1$^+$ myeloid cell infiltration and inhibits HCC growth. Similarly, antibody blockade of Gr-1 reduces tumor fibrosis and inhibits HCC growth when combined with sorafenib treatment. *Conclusion*: Blocking SDF-1α/CXCR4 or Gr-1$^+$ myeloid cell infiltration may reduce hypoxia-mediated HCC desmoplasia and increase the efficacy of sorafenib treatment. (HEPATOLOGY 2014;59:1435-1447)

Abbreviations: Ab, antibody; Ad-Cre, Cre-expressing adenovirus; AKT, protein kinase B; APC, allophycocyanin; CAIX, carbonic anhydrase IX; CXCL12, C-X-C ligand 12; CXCR4, C-X-C receptor type 4; DAPI, 4′,6-diamidino-2-phenylindole; ECM, extracellular matrix; ERK, extracellular signal-related kinase; FCM, flow cytometry; FGFR, basic fibroblast growth factor receptor; Gr-1, myeloid differentiation antigen; HCC, hepatocellular carcinoma; HSC, hepatic stellate cell; IHC, immunohistochemical; IV, intravenous; 5-LO, 5-lipoxygenase; MAPK, mitogen-activated protein kinase; MCP-1, monocyte chemoattractant protein-1; MMP, matrix metalloproteinase; MTT, 3-[4,5-dimethylthiazol-2-yl]-2,5-diphenyl tetrazolium bromide; p-AKT, phosphorylated AKT; PBS, phosphate-buffered solution; PCR, polymerase chain reaction; PDGFR, platelet-derived growth factor receptor; p-ERK, phosphorylated ERK; r, recombinant; SDF-1α, stromal-derived factor 1 alpha; siRNA, small interfering RNA; α-SMA, alpha smooth muscle actin; TGF, transforming growth factor; TKI, tyrosine kinase inhibitor; VEGF, vascular endothelial growth factor; VEGFR, vascular endothelial growth factor receptor.

From the [1]Steele Laboratory for Tumor Biology, Department of Radiation Oncology; [2]Department of Pathology; and [3]Department of Medicine, Massachusetts General Hospital, Harvard Medical School, Boston, MA.

Received July 14, 2013; accepted October 3, 2013.

This study was supported by the National Institutes of Health grants no.: P01-CA080124, R01-CA159258, R21-CA139168, R01-CA126642 and National Cancer Institute/Proton Beam Federal Share Program awards (to D.G.D. and R.K.J.), by the American Cancer Society grant 120733-RSG-11-073-01-TBG (to D.G.D.) and by a Max Kade Fellowship (to T.R.).

Hepatocellular carcinoma (HCC) almost exclusively arises in cirrhotic livers as well as preexisting chronic inflammation and fibrosis fuel hepatocarcinogenesis and HCC growth.[1-3] Fibrosis is the consequence of hepatic stellate cell (HSC) activation and proliferation as well as myofibroblast differentiation leading to increased collagen deposition.[4] This dual pathology of the liver contributes to an aggressive, systemic treatment-refractory characteristic in HCCs.[1] Recently, the tyrosine kinase inhibitor (TKI), sorafenib, has emerged as the first systemic therapy for HCC. Sorafenib is an antiangiogenic drug that has a broad tyrosine kinase inhibition spectrum.[5] However, despite this progress, the mortality rate from HCC remains high, making this disease the third-leading cause of cancer-related death worldwide.[6-10]

Sorafenib is widely considered as an antiangiogenic/-vascular drug through inhibition of vascular endothelial growth factor (VEGF) receptors (VEGFRs) and platelet-derived growth factor receptors (PDGFRs). However, more-potent and -selective anti-VEGF agents or more-broad antiangiogenic agents (e.g., VEGFR/basic fibroblast growth factor receptor [FGFR] and anti-VEGFR/PDGFR inhibitors) have thus far failed to match the efficacy of sorafenib in phase III trials in HCC.[10-13] Moreover, antiangiogenic therapy has not led to tumor regression in patients or in experimental models in mice: The benefit noted with sorafenib in HCC patients is likely the result of a transient delay in HCC growth, after which most tumors resume their growth.[10] Whereas the mechanisms of acquired resistance to sorafenib and other anti-VEGF inhibitors in HCC remain unknown, it is likely that tumor stroma-mediated survival pathways might play a key role.[1,10] Of these, increased hypoxia has been proposed as a mechanism of resistance to multitargeted TKI therapy.[14-17] The challenge is to identify the key molecular pathways regulating stroma-mediated resistance to sorafenib treatment in HCC.

Hypoxia and other cellular stresses can promote the expression of the chemokine, stromal-derived factor 1 alpha (SDF-1α or C-X-C ligand 12 [CXCL12]), and of its receptor, C-X-C receptor type 4 (CXCR4).[18-22] In clinical studies, we showed that SDF-1α level increased in plasma circulation in HCC patients after treatment with sunitinib or cediranib (both anti-VEGFR and anti-PDGFR TKIs).[23,24] Moreover, we showed that elevated circulating levels of SDF-1α correlated with poor treatment outcome in HCC patients after sunitinib treatment.[23] Systemic activation of the SDF-1α/CXCR4 axis is known to mediate intratumoral infiltration of inflammatory cells, including myeloid differentiation antigen–positive ($Gr\text{-}1^+$) myeloid ($CD11b^+$) cells.[25-28] $Gr\text{-}1^+$ myeloid cells can drive tumor recurrence after anti-VEGF therapy in various tumor models.[29] Finally, clinical correlative data also strongly suggest that the effects on multitargeted TKI treatment on tumor vasculature and myeloid cells may mediate response and resistance therapy in HCC patients.[23,30] However, a causal role of $Gr\text{-}1^+$ myeloid cells in HCC resistance to antiangiogenic treatment has not been characterized. Furthermore, a mechanistic understanding of the interplay between treatment-induced hypoxia, SDF-1α/CXCR4 pathway activation, and $Gr\text{-}1^+$ myeloid cell infiltration and tumor fibrosis in HCC is currently lacking. Here, we examined, in orthotopic HCC models, whether the SDF-1α/CXCR4 pathway is activated and causally related to $Gr\text{-}1^+$ myeloid cell infiltration and tumor-associated fibrosis and, ultimately, to sorafenib resistance.

Materials and Methods

Cells and Materials. We used the C3H mouse-derived HCC cell line, HCA-1.[31] Human HSCs

Yunching Chen is currently affiliated with the Institute of Biomedical Engineering, National Tsing Hua University, Hsinchu City, Taiwan.
Annique M. Duyverman is currently affiliated with the Universty of Utrecht, Utrecht, the Netherlands.
Rekha Samuel is currently affiliated with Christian Medical College, Vellore, India.
Lotte Hiddingh is currently affiliated with VU University Medical Center, Amsterdam, the Netherlands.
Address reprint requests to: Dan G. Duda, D.M.D., Ph.D., Steele Laboratory for Tumor Biology, Massachusetts General Hospital, Cox-734, 100 Blossom Street, Boston, MA 02114. E-mail: duda@steele.mgh.harvard.edu; fax: 617-726-1962.

View this article online at wileyonlinelibrary.com.
DOI 10.1002/hep.26790
Potential conflict of interest: Stock Ownership – R.K.J., SynDevRx, Enlight, XTuit; Employment or Leadership Position – none; Consulting – R.K.J., Enlight, Noxxon, Zyngenia, D.G.D., Hexal/Sandoz, A.X.Z., Sanofi-Aventis, Eisai, Exelixis; Advisory arrangements – T.R., MSD, Gilead; Speakers' Bureau – none; Grants/Contracts: Research – T.R., Roche, Phenex, MSD, Gilead, Janssen, R.K.J., Dyax, MedImmune, Roche, A.X.Z., Bayer, Onyx, Lilly; Grants/Contracts: Unrestricted – none; Travel Grants – T.R., Roche, MSD, Gilead, Janssen; Intellectual Property Rights – none; Other Interests – R.K.J., Board of Directors of XTuit and Boards of Trustees of H&Q Healthcare Investors and H&Q Life Sciences Investors.
Additional Supporting Information may be found in the online version of this article.

(catalog no.: 5300) were purchased from ScienCell Research Laboratories (San Diego, CA). These primary HSCs have been previously characterized.[32] We purchased AMD3100 and FR180204 from Sigma-Aldrich (St. Louis, MO), AZD6244 and sorafenib from Selleck Chemicals (Houston, TX), recombinant PDGF-B and SDF-1α from R&D Systems (Minneapolis, MN), and anti-Gr-1 antibody (Ab; Leaf purified anti-mouse Gr-1 Ab) from BioLegend, Inc. (San Diego, CA). For coculture experiments, we isolated Gr-1$^+$ myeloid cells from enzymatically digested HCA-1 tumors.

Animals. To induce liver fibrosis, we treated 5-week-old male C3H or *Mst1*$^{-/-}$*Mst2*$^{F/-}$ mice with CCl_4 (16% [v/v] in olive oil, 100-μL gavage, 3 times per week) before tumor implantation and induction. HCA-1 cells were orthotopically implanted in mice 2 weeks after the last CCl_4 treatment, as previously described.[33] *Mst1*$^{-/-}$*Mst2*$^{F/-}$ mice develop spontaneous HCCs after intravenous (IV) injection of Cre-expressing adenovirus (Ad-Cre)[34] and were a kind gift from Dr. Nabeel Bardeesy (Massachusetts General Hospital, Boston, MA). All animals received humane care according to the criteria outlined in the "Guide for the Care and Use of Laboratory Animals" prepared by the National Academy of Sciences and published by the National Institutes of Health (publication 86-23, revised 1985).

Treatment Studies. Mice were treated daily by gavage with sorafenib (40 mg/kg) or vehicle (phosphate-buffered saline; PBS) alone. AMD3100 (10 mg/kg/day) was delivered continuously using Alzet microosmotic pumps (DURECT Corporation, Cupertino, CA) over 2 weeks.

Cell Viability Assays. We assessed cell viability using the 3-[4,5-dimethylthiazol-2-yl]-2,5-diphenyl tetrazolium bromide (MTT) assay (Sigma-Aldrich).

Western Blotting Analysis. Western blotting was performed using Abs against collagen I and alpha-smooth muscle actin (α-SMA; Abcam, Cambridge, MA) as well as phosphorylated (p-) extracellular signal-related kinase (p-ERK), ERK, phosphorylated (p-) protein kinase B (p-AKT), and AKT (Cell Signaling Technology, Danvers, MA).

Small Interfering RNA Knockdown. ON-TARGETplus CXCR4 small interfering RNA (siRNA) and nontargeting control siRNA were purchased from Dharmacon (Lafayette, CO) and used for transfection of HCA-1 cells.

Immunohistochemistry. For murine samples, we used Abs against α-SMA, carbonic anydrase IX (CAIX; Abcam), collagen I (LF-67; kindly provided by Dr. L. Fisher, National Institute of Dental and Craniofacial Research, Bethesda, MD), and SDF-1α (BioVision, Inc., Milpitas, CA). For apoptosis detection, frozen tumor sections were stained using the TACS TdT Kit (R&D Systems). To assess expression level, we measured the fluorescently stained area for each marker and normalized it to the 4′,6-diamidino-2-phenylindole (DAPI) area (used as a measure of cellularity in viable tumor regions), as previously described.[28] In addition, we performed immunostaining for SDF-1α in tumor samples from patients who underwent HCC resection. Hepatic fibrosis in the non-HCC liver area was evaluated according to the Laennec system, as previously described.[35] Colocalization between SDF-1α expression and desmoplasia was assessed in 10 randomly selected high-power fields at 4× magnification.

Flow Cytometry. We used fluorescently labeled rat monoclonal Abs anti-mouse CD45/phycoerythrin/Cy7, Gr-1/allophycocyanin (APC), and CD11b/APC/Cy7 (BD Biosciences, San Jose, CA) to perform flow cytometric (FCM) analysis in digested tumor tissue, as previously described.[36]

Quantitative Reverse-Transcription Polymerase Chain Reaction. We determined relative gene expression of SDF-1α, CXCR4, monocyte chemoattractant protein 1 (MCP-1), 5-lipoxygenase (5-LO), transforming growth factor (TGF)-α, TGF-β, PDGF-α, PDGF-β, matrix metalloproteinase (MMP)−9, MMP-13, and β-actin in tumor-infiltrating Gr-1+ cells using specific primers (Supporting Table 1), Real-Time SYBR Green PCR master mix (Applied Biosystems, Branchburg, NJ) and the Stratagene Mx3000P QPCR System, as previously described.[36]

Statistical Analysis. Comparisons between treatment groups were performed using Mann-Whitney's U-test. A P value of less than 0.05 was considered to denote statistical significance.

Further details on materials and methods used are described in the Supporting Experimental Methods section of the Supporting Materials.

Results

Sorafenib Treatment Increases Hypoxia and SDF-1α Expression in Orthotopic HCC Models. To model the clinical features of HCC, we first induced liver fibrosis in mice by CCl_4 treatment for 11 weeks (Supporting Fig. 1). Then, we generated orthotopic tumors by intrahepatic HCA-1 cell implantation in C3H mice or by inducing spontaneous HCC using Ad-Cre IV injection in *Mst1*$^{-/-}$*Mst2*$^{F/-}$ mice (Supporting Fig. 2). When tumors became established, we treated mice with sorafenib for 14 days and then measured the

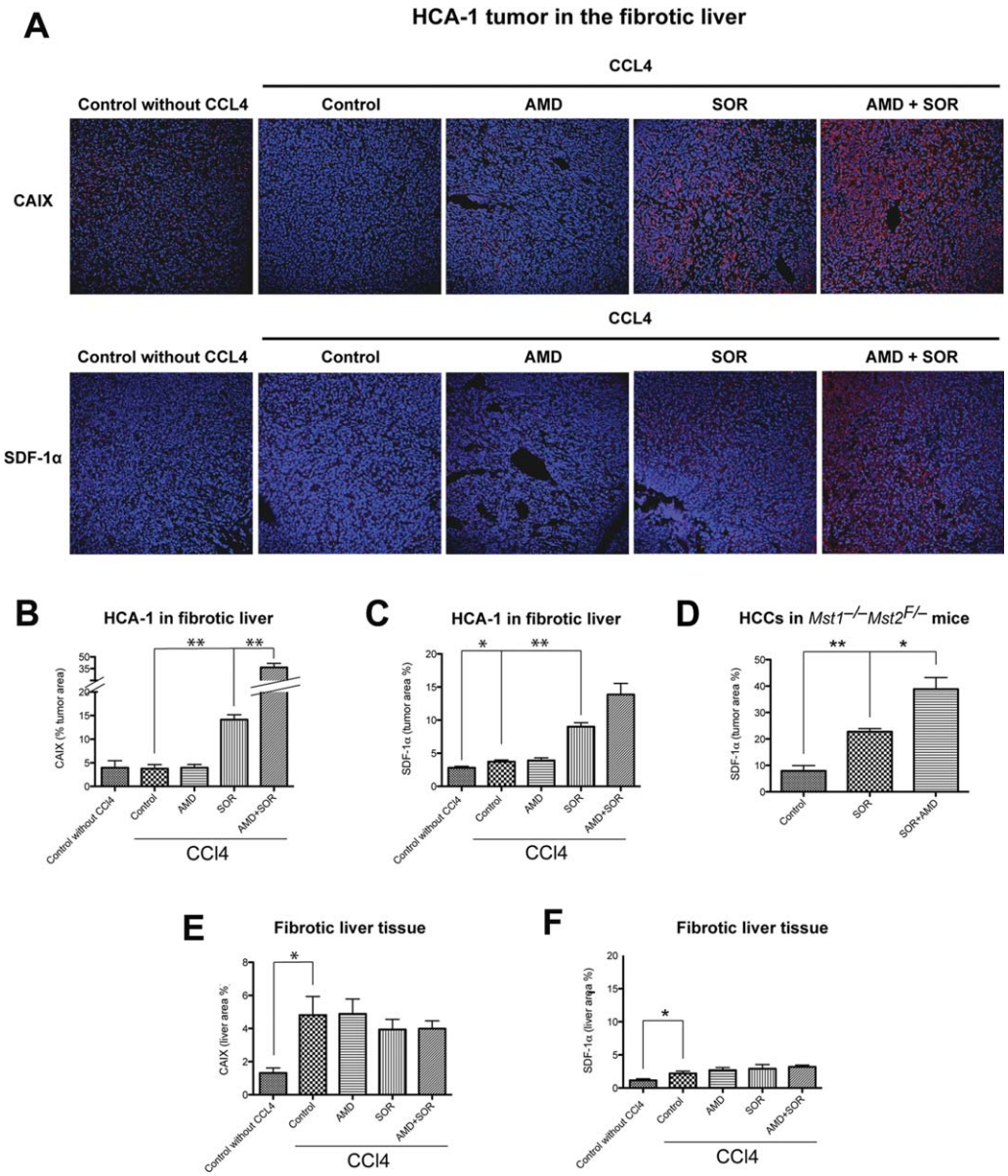

Fig. 1. Tumor hypoxia and SDF-1α expression are increased after sorafenib treatment in orthotopic HCC. (A) Representative immunofluorescence staining of CAIX and SDF-1α in HCA-1 tumor-implanted in mice with liver fibrosis. Images are 636 μm across. (B and C) Hypoxic tumor tissue fraction (B) and SDF-1α expression (C) increased significantly after sorafenib treatment in orthotopic HCA-1 tumors in mice (n = 5-9). (D) Immunofluorescence imaging analysis showed that SDF-1α expression is increased after 14 days of sorafenib treatment in spontaneous HCCs in $Mst1^{-/-}Mst2^{F/-}$ transgenic mice. Increased hypoxia and SDF-1α expression persisted when sorafenib treatment was combined with AMD3100 (n = 5-9). (E and F) Expression of CAIX (E) and SDF-1α (F) in the liver was not significantly changed after sorafenib, AMD3100, or combination treatment (n = 4-7). The number of random regions of interest used for quantification is shown in parentheses. Data are presented as mean ± standard error of the mean. $*P < 0.05$; $**P < 0.01$.

changes in tissue oxygenation. Sorafenib treatment significantly increased the hypoxic tissue fraction—measured by CAIX immunostaining—when compared to control-treated tumors (Fig. 1A,B). In contrast, hypoxic tissue surface area did not increase in surrounding fibrotic liver tissue after treatment (Fig. 1E).

To examine the consequence of treatment-induced increase in tumor hypoxia, we next evaluated whether the increase in SDF-1α expression—suggested by studies in HCC patients[23,24]—is recapitulated in these HCC models. Indeed, we found a 2-fold elevation in SDF-1α expression after sorafenib treatment in HCA-1 tumor grafts and in spontaneous HCCs in $Mst1^{-/-}Mst2^{F/-}$ mice (Fig. 1A-D and Supporting S3). In contrast, SDF-1α expression did not significantly increase in the fibrotic liver after sorafenib treatment (Fig. 1F).

To confirm that hypoxia is the driver of SDF-1α expression in cancer and stromal cells, we cultured

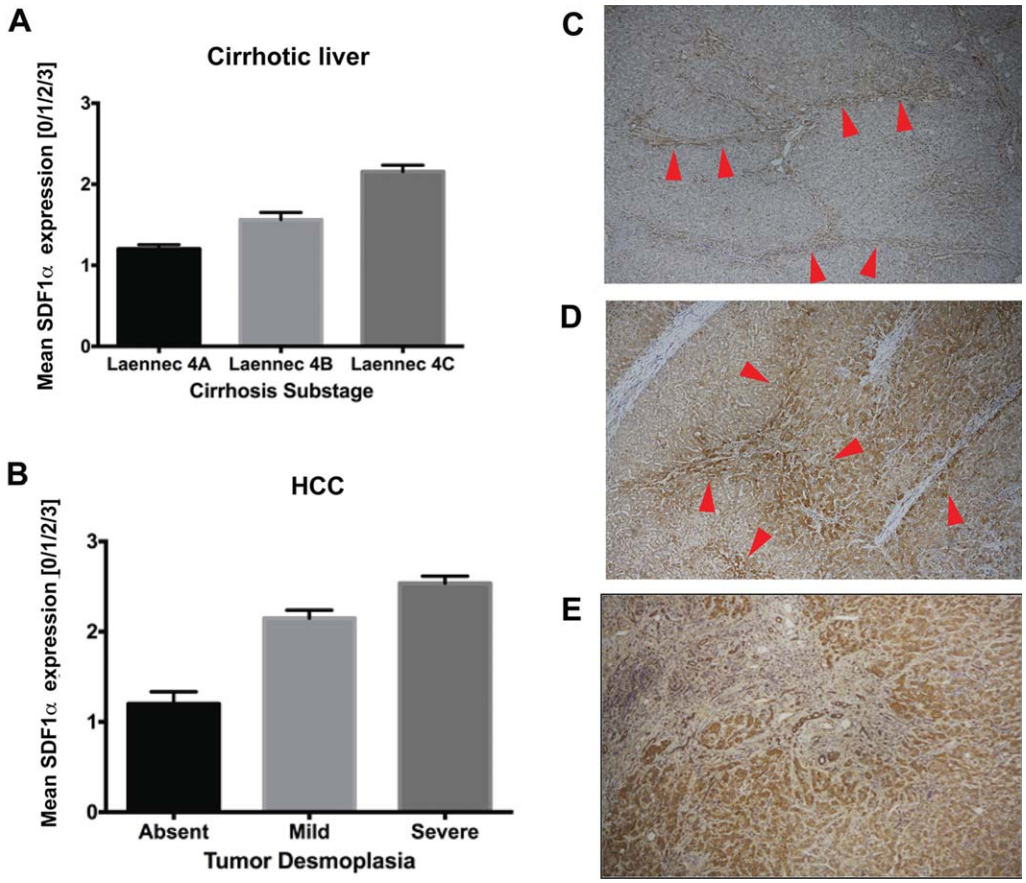

Fig. 2. Immunostaining for SDF-1α in liver tissue samples from HCC patients. Paraffin-embedded tissue sections were stained for SDF-1α by IHC. (A and B) SDF-1α expression in nonmalignant liver tissue (A) was consistently lower than in the malignant HCC tumor area (B). Both in cirrhotic liver tissue (C) and in HCC nodules (D), SDF-1α expression was colocalized with ECM components/fibrous septa supporting the potential profibrotic role of SDF-1α in human hepatic fibrogenesis and HCC desmoplasia. (E) Specimens of tumors that reoccurred after transcatheter arterial chemoembolization and radiofrequency ablation—both of which are known to cause severe hypoxia—consistently showed high expression of SDF-1α, which was also associated with more pronounced desmoplasia in the HCC area. Error bars represent score ± standard error of the mean (n = 10 regions of interest per sample).

HCA-1 cells as well as HSCs for 48 hours in hypoxic (1% O_2) or normoxic (21% O_2) conditions and measured SDF-1α expression by quantitative polymerase chain reaction (PCR). Exposure to hypoxic conditions increased SDF-1α expression in both HCC cells and HSCs (Supporting Fig. 4).

To evaluate the effect of SDF-1α/CXCR4 pathway inhibition on tumor tissue oxygenation and SDF-1α expression after treatment, we combined sorafenib treatment with the CXCR4 inhibitor, AMD3100 (10 mg/kg/day; Sigma-Aldrich). Interestingly, the combination therapy further increased hypoxic tissue fraction and SDF-1α expression in orthotopic HCA-1 tumor grafts and spontaneous HCCs in *Mst1*$^{-/-}$*Mst2*$^{F/-}$ mice, when compared to sorafenib treatment alone (Fig. 1 and Supporting Fig. 3).

***Inhibition of CXCR4 Prevents the Increase in HCC Fibrosis After Sorafenib* In Vivo.** To establish whether fibrosis is associated with elevated SDF-1α expression in HCC patients, we examined surgical specimens for HCC patients with cirrhosis. We observed that SDF-1α expression colocalized with extracellular matrix (ECM) components and fibrotic septa in both HCC and cirrhotic liver tissues (Fig. 2). Thus, we next evaluated the effect of sorafenib treatment with or without inhibition of SDF-1α/CXCR4 pathway on fibrosis, a hallmark of HCC progression,[4] in the mouse models. To this end, we measured expression of collagen I as well as the number of α-SMA$^+$ myofibroblasts after sorafenib treatment, both in the tumor region and in surrounding liver tissue. Of note, the α-SMA$^+$ myofibroblasts were also positive for glial fibrillary acidic protein (Supporting Fig. 5). Immunohistochemical (IHC) analyses revealed that the HCCs growing in the face of sorafenib treatment showed significantly increased tumor desmoplasia. Treatment resulted in increased intra- and peritumoral collagen I and α-SMA$^+$ myofibroblast

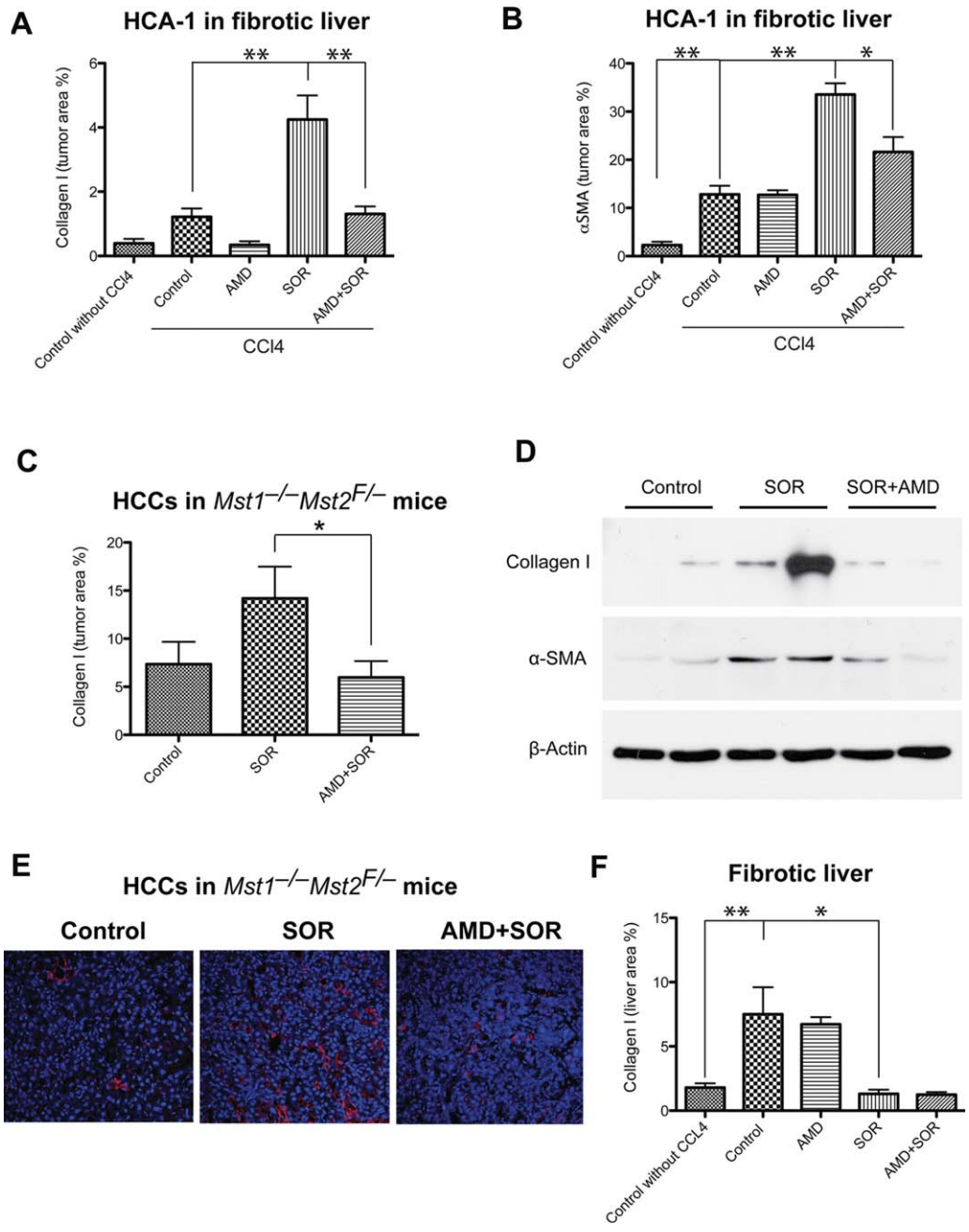

Fig. 3. Sorafenib treatment selectively increases tumor-associated fibrosis in HCC in an SDF-1α/CXCR4 pathway-dependent manner. (A and B) Sorafenib significantly increased collagen I content (A) and the number of α-SMA$^+$ myofibroblasts (B) in orthotopic HCA-1 tumors implanted in mice with fibrotic livers. Analysis was performed using immunofluorescence in tumor tissue, and the maker-positive area was normalized to the area of DAPI (nuclear stain; N = 5-7). (C and D) Sorafenib treatment significantly increased collagen I content (C and D) and expression of α-SMA (D) (detected by western blotting) in spontaneously arising HCCs (N = 7-8). (E) Representative images of immunofluorescence of collagen I staining in spontaneous HCCs. Images are 636 μm across. Addition of AMD3100 to sorafenib treatment prevented the increase in collagen I content and the number of α-SMA$^+$ myofibroblasts in HCCs (A-E). (F) In tumor-bearing mice, sorafenib significantly reduced collagen I content in surrounding liver tissue in mice with underlying liver fibrosis to levels comparable to those noted in livers from non-CCl_4-treated mice (N = 4-8). The number of random regions of interest used for quantification is shown in parentheses. *$P < 0.05$; **$P < 0.01$. Data are shown as mean ± standard error of the mean.

infiltration in orthotopic HCA-1 HCCs in mice with CCl_4-induced liver fibrosis and in spontaneous HCCs in *Mst1*$^{-/-}$*Mst2*$^{F/-}$ mice (Fig. 3A-E). Of note, sorafenib treatment reduced collagen I expression levels in surrounding liver tissue in mice with CCl_4-induced liver fibrosis (Fig. 3F).

To assess the effect of SDF-1α/CXCR4 pathway inhibition on tumor-associated fibrosis after sorafenib

treatment, we tested the combined administration of sorafenib with the CXCR4 inhibitor, AMD3100. This combination therapy prevented the increase in collagen I expression and α-SMA$^+$ myofibroblasts after sorafenib treatment in spontaneous and implanted HCCs, without significantly changing collagen I expression in fibrotic liver in CCl_4-treated mice (Fig. 3). Of note, this effect was observed despite a persistent increase in hypoxia and SDF-1α expression in the HCCs treated with sorafenib and AMD3100 (Fig. 1A-D). Thus, CXCR4 inhibition can prevent the profibrotic effects of sorafenib treatment in HCC *in vivo*, despite persistent tumor hypoxia.

SDF-1α/CXCR4 Axis Directly Mediates HSC Differentiation to Myofibroblasts in HCC Despite PDGFR Blockade by Sorafenib. Next, we examined the role of the SDF-1α/CXCR4 axis in selective promotion of tumor fibrosis after sorafenib treatment *in vitro*. To determine whether increased SDF-1α expression in tumor could mediate the increase in tumor fibrosis after sorafenib treatment, we first exposed primary HSCs to recombinant (r)SDF-1α in the presence or absence of sorafenib or rPDGF-B. Consistent with previous reports,[37] we found that rPDGF-B stimulated proliferation and α-SMA expression in HSCs (Fig. 4A,B). Sorafenib treatment prevented the effects of rPDGF-B and led to significant decrease in HSC viability (as evidenced by an increase in cleaved caspase-3 expression and in the number of apoptotic HSCs) and inhibited α-SMA and collagen I expression (Fig. 4A-C). These results indicate that sorafenib treatment may directly reduce liver fibrosis by blocking the PDGFR pathway in HSCs. Exposure to rSDF-1α induced HSC differentiation into myofibroblasts, as evidenced by dose-dependent increases in α-SMA and collagen I expression as well as in ERK and Akt activation (Fig. 4D). Then, we evaluated whether SDF-1α can drive HSC differentiation and activation of HSCs in the face of PDGFR blockade by sorafenib treatment. We found that SDF-1α increased cell proliferation and viability as well as promoted the differentiation of HSCs, despite sorafenib treatment (Fig. 4A-C).

Finally, to determine whether the SDF-1α/CXCR4 axis mediates these effects in HSCs, we used pharmacologic and genetic approaches to inhibit CXCR4. To this end, we cultured HSCs in the presence of rSDF-1α with or without the CXCR4 inhibitor, AMD3100, or with or without CXCR4 expression knockdown using siRNA. In both settings, inhibition of CXCR4 prevented the effects of SDF-1α on HSC differentiation and activation (i.e., prevented the increase in α-SMA and collagen I expression induced by SDF-1α in HSCs; Fig. 4D,E and Supporting Fig. 6). Inhibitory effects were mediated, in part, by preventing activation of mitogen-activated protein kinase (MAPK) pathway activation by SDF-1α, as shown by ERK inhibition with FR180204 (2 μM) or MAPK kinase inhibition with AZD6244 in HSCs treated with rSDF-1α (Fig. 4D-F and Supporting Fig. 7).

Gr1$^+$ Myeloid Cell Infiltration Increases in HCC AFTER Sorafenib in an SDF-1α/CXCR4-Dependent Manner. Next, we examined the effects of treatment with sorafenib—with or without inhibition of CXCR4—on inflammatory cell infiltration in HCC. To this end, we evaluated enzymatically digested HCC tissue by FCM analysis. We found that the number of Gr-1$^+$ myeloid cells increased by over 2-fold in HCA-1-transplanted HCC models and in spontaneous HCCs in *Mst1*$^{-/-}$*Mst2*$^{F/-}$ mice after sorafenib treatment (Fig. 5A,B). In contrast, we found that sorafenib treatment reduced the accumulation of Gr-1$^+$ myeloid cells in surrounding fibrotic liver tissue (Fig. 5C). Finally, inhibition of CXCR4, using AMD3100 in combination with sorafenib, decreased the number of tumor-infiltrating Gr-1$^+$ myeloid cells to levels comparable to control-treated spontaneous and transplanted HCCs (Fig. 5A,B).

Gr1$^+$ Myeloid Cell Infiltration Increases Fibrosis in HCC After Sorafenib in a SDF-1α/CXCR4-Dependent Manner. Next, we tested whether direct Gr-1$^+$ myeloid cell blockade could prevent the increase in fibrosis after sorafenib treatment in HCC. To achieve this, we used an anti-Gr-1-blocking Ab with or without sorafenib treatment in mice with CCl_4-induced liver fibrosis with orthotopically implanted HCA-1 tumors. Gr-1 blockade prevented the increase in Gr-1$^+$ myeloid cell infiltration in HCC after sorafenib treatment to levels comparable to tumors from control-treated mice (Fig. 6A). Moreover, inhibition of Gr-1$^+$ myeloid cell infiltration also prevented the increase in HCC-associated fibrosis observed after sorafenib treatment (i.e., decreased the levels of collagen I and α-SMA expression; Fig. 6B,C). To examine the mechanisms by which Gr-1$^+$ myeloid cells promote fibrosis, we isolated HCC-infiltrating Gr-1$^+$ (Ly-6G/Ly-6C) myeloid cells from HCA-1-digested tumor tissue by way of magnetic separation and cocultured them with HSCs—either with or without direct contact. In both coculture systems, Gr-1$^+$ cells stimulated collagen I and α-SMA expression (measured in HSCs) in a dose-dependent manner (Fig. 6D and Supported Fig. 8A). This indicates that soluble factors released by Gr-1$^+$ myeloid cells promote fibrosis. To determine whether the effects of Gr-1$^+$

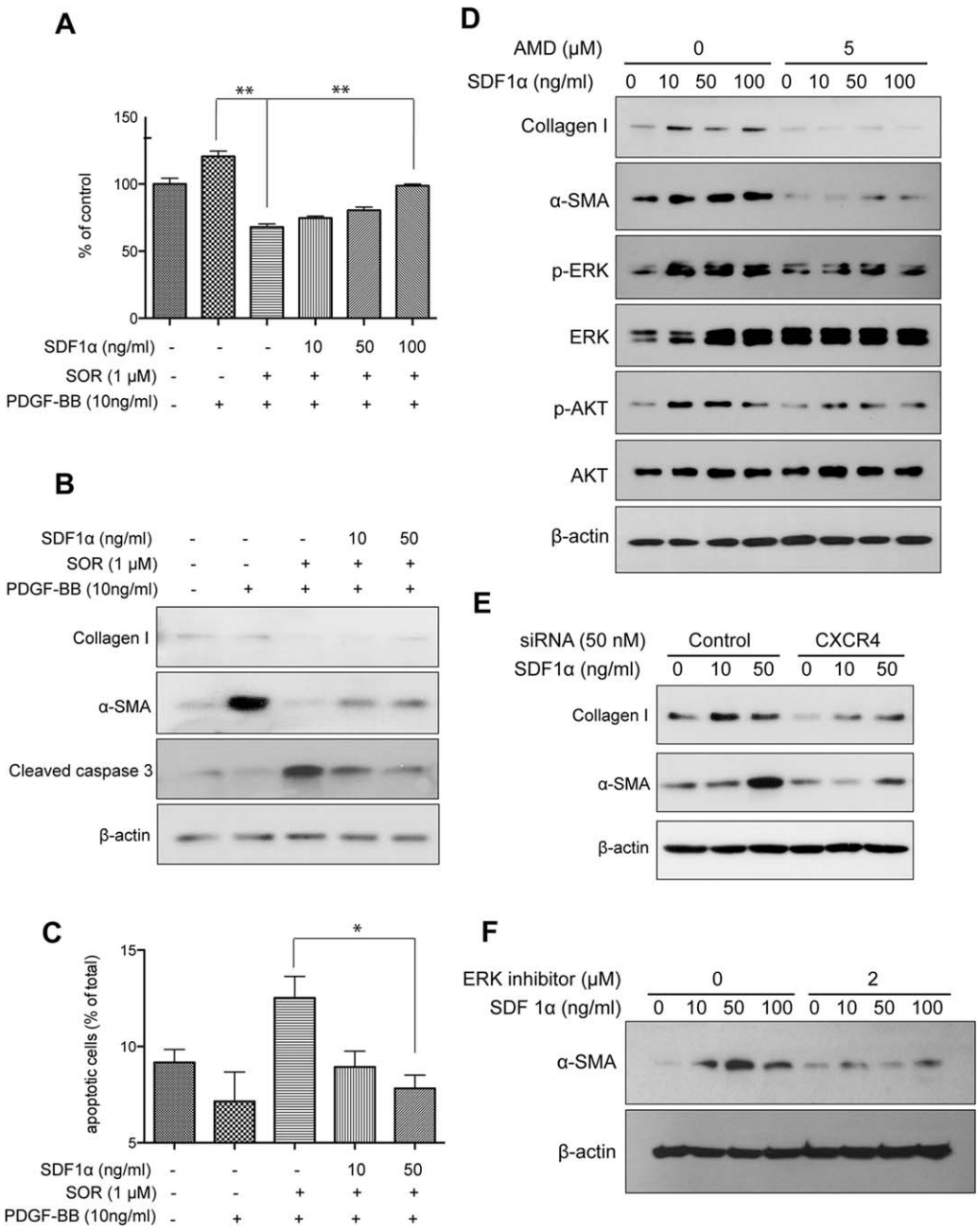

Fig. 4. SDF-1α/CXCR4 axis promotes HSC to myofibroblast differentiation in the face of PDGFR blockade by sorafenib. (A) Exposure to rPDGF-B increased HSC proliferation, whereas treatment with sorafenib reduced the viability of HSCs. Exposure to recombinant SDF1-α increased the viability of HSCs, despite PDGFR inhibition using sorafenib treatment, in a dose-dependent manner. HSC viability was measured by MTT assay (N = 6 experimental repeats). (B) Exposure to rSDF-1α increased expression of α-SMA and collagen I and reduced cleaved caspase-3 expression (evaluated by western blotting), despite sorafenib treatment, in a dose-dependent manner. (C) Exposure to rSDF-1α increased viability of HSCs, despite sorafenib treatment (N = 3-5 experimental repeats). (D) Exposure to rSDF-1α up-regulated collagen I and α-SMA expression levels as well as ERK and AKT activation in HSCs, consistent with their myofibroblast differentiation. Inhibition of CXCR4 with AMD3100 (D) or using siRNA (E) prevented the effects of SDF-1α. (F) ERK inhibition with FR-180204 (2 μM) decreased α-SMA expression in HSCs treated with rSDF-1α. Data are presented as mean ± standard error of the mean.

myeloid cells on HSCs can overcome PDGFR blockade by sorafenib, we repeated the coculture experiments in the presence or absence of sorafenib and rPDGF-B. We found that Gr-1$^+$ myeloid cells can drive, in a dose-dependent manner, HSC differentiation and activation despite effective blockade of PDGFR by sorafenib treatment (Fig. 6E and Fig. S8B). To examine the profibrotic factors involved in this paracrine interaction, we sorted Gr1$^+$ myeloid cells from digested HCC tissue from mice treated with

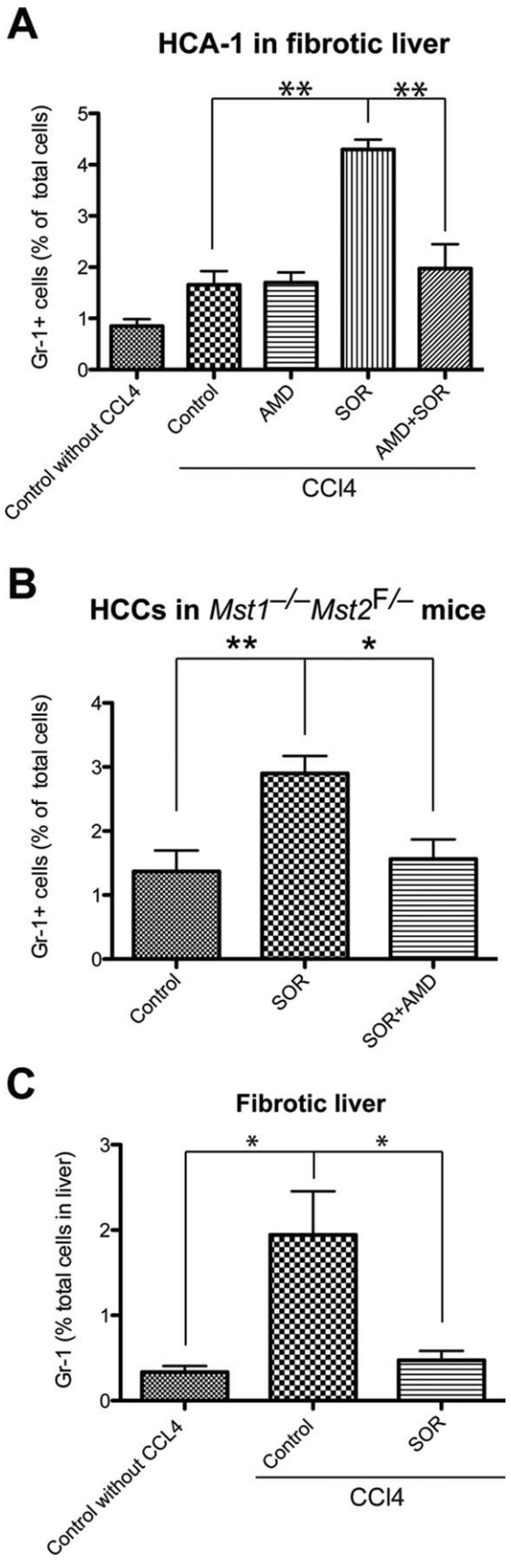

sorafenib or vehicle control and then extracted messenger RNA. We next performed real-time PCR analysis to measure expression of profibrotic cytokines.[4] Gr-1$^+$ myeloid cells from sorafenib-treated tumors showed higher expression of several profibrotic factors (5-LO, PDGF-B, and MCP-1 as well as of SDF-1α and CXCR4), compared to Gr-1$^+$ myeloid cells from control-treated tumors (Supporting Table 2). To evaluate whether the SDF-1α/CXCR4 axis mediates not only Gr-1$^+$ myeloid cell infiltration in HCC, but also their paracrine interaction with HSCs leading to fibrosis, we inhibited CXCR4 with AMD3100 in the coculture systems described above. AMD3100 treatment prevented the up-regulation of collagen I and α-SMA expression in HSCs cocultured with tumor-derived Gr-1$^+$ myeloid cells in a dose-dependent manner (Fig. 6F). Taken together, these data show that the SDF-1α/CXCR4 pathway mediates both the increased infiltration of Gr-1$^+$ myeloid cells in HCC by sorafenib treatment as well as their profibrotic effects on HSCs.

Inhibition in CXCR4 or Gr-1 in Combination With Sorafenib Inhibits HCC Growth, Compared to Sorafenib Alone. Finally, given the SDF-1α mediation of profibrotic and -inflammatory effects in HCC after sorafenib treatment, we next evaluated the specific effect of fibrosis on HCC growth after treatment with sorafenib or the CXCR4 inhibitor, AMD3100. First, we found that the growth of spontaneous and grafted HCC was accelerated in mice with fibrotic liver, compared to mice with normal liver (Fig. 7A and Supporting Fig. 2). AMD3100 treatment alone showed no significant inhibition of HCC growth. However, when combined with sorafenib, AMD3100 induced a significant additional tumor growth inhibition of orthotopic HCA-1 tumors in immunocompetent C3H mice with underlying liver fibrosis (Fig. 7A). Moreover, inhibition of CXCR4 with AMD3100 in combination with sorafenib induced a significant increase in cell apoptosis, compared to sorafenib or AMD3100 alone, in both

Fig. 5. Intratumoral infiltration of Gr1$^+$ myeloid cells is increased after sorafenib (SOR) treatment and is prevented by CXCR4 inhibition in HCC. (A and B) After SOR treatment, the number of 7-Aminoactinomycin D (7-AAD)/CD11b$^+$Gr1$^+$ monocytes (measured by FCM) significantly increased in HCA-1 tumors growing in C3H mice with liver fibrosis (A) as well as in spontaneous HCCs in *Mst1*$^{-/-}$*Mst2*$^{F/-}$ transgenic mice (B). Treatment with the CXCR4 inhibitor, AMD3100, prevented this effect (A and B). (C) The number of 7-AAD/CD11b$^+$Gr1$^+$ myeloid cells was significantly reduced in fibrotic liver tissues from sorafenib-treated mice. Data are shown as percentages of the total number of cells evaluated in enzymatically digested tissue. Data are presented as mean ± standard error of the mean (N = 5-14 mice per group). **P < 0.01.

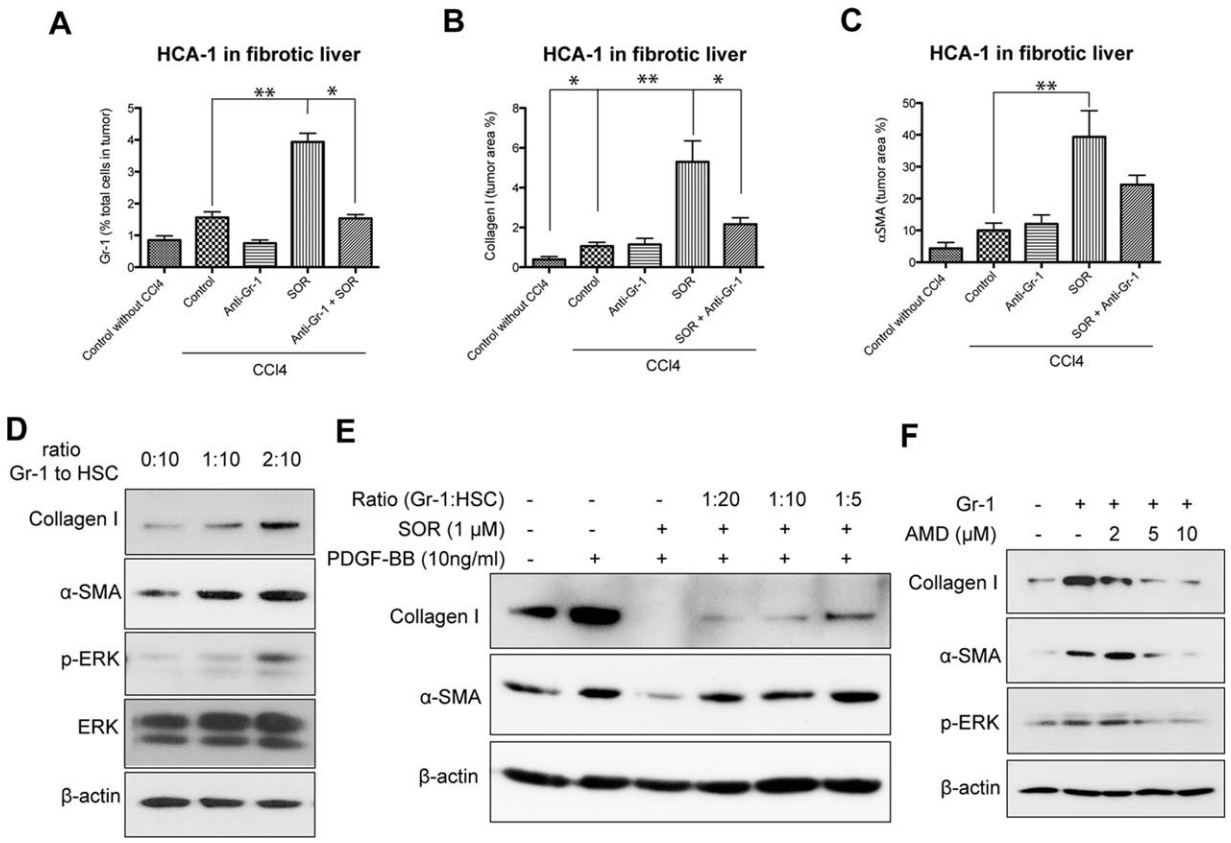

Fig. 6. Gr-1$^+$ myeloid cell infiltration increases fibrosis in HCC after sorafenib in an SDF-1α/CXCR4 pathway-dependent manner. (A-C) Depletion of Gr-1$^+$ myeloid cells using systemic therapy with anti-Gr-1-blocking Abs prevents the shift toward a profibrotic environment after sorafenib treatment. Sorafenib significantly increased the number of 7-AAD/CD11b$^+$Gr1$^+$ monocytes (A) (N = 3-7 mice per group), collagen I content (B), and number of α-SMA$^+$ myofibroblasts (C) in orthotopic HCA-1 tumors growing in mice with liver fibrosis evaluated by IHC. Combining anti-Gr-1 Abs with sorafenib treatment prevented these effects. Quantification was performed in 5-12 confocal microscopy images per mouse. (D-F) Tumor-infiltrating Gr-1$^+$ myeloid cells directly mediated HSC differentiation to myofibroblasts through the SDF-1α/CXCR4 axis. Coculture with tumor-tissue–isolated Gr1$^+$ myeloid cells (obtained using magnetic beads) increased collagen I and α-SMA expression levels as well as ERK activation in HSCs (D). Coculture with Gr1$^+$ myeloid cells increased collagen I and α-SMA expression in HSCs, despite sorafenib treatment, in a dose-dependent manner (E). rPDGF-B and sorafenib alone were used as positive and negative control, respectively, for HSC differentiation (E). Inhibition of CXCR4 with AMD3100 prevented the increase in collagen I, α-SMA, and p-ERK expression in HSCs cocultured with Gr-1$^+$ myeloid cells (F). Data are presented as mean ± standard error of the mean. *$P < 0.05$.

grafted and spontaneous orthotopic HCC models (up to 20% in HCA-1 growing in fibrotic liver; Fig. 7B-E). Of note, the liver function parameters (alanine aminotransferase, aspartate aminotransferase, and alkaline phosphate) remained unchanged after combination treatments (not shown). Finally, combination of anti-Gr-1 Ab with sorafenib also induced a significant delay in HCC growth, compared to sorafenib alone (Fig. 7F).

Discussion

Despite its inhibitory effect on hepatic fibrogenesis, the efficacy of sorafenib treatment in HCC may be thwarted by the ensuing increase in hypoxia that leads to increased tumor desmoplasia and inflammation. We show that although sorafenib can reduce chemically induced liver fibrosis in mice, its antivascular effects in tumors lead to increased hypoxia, inflammation, and fibrosis in tumor tissue. Our results confirm the antifibrotic effects observed in cirrhotic livers with sorafenib and other TKIs (vatalanib),[38,39] but also reveal that tumor-associated fibrosis/desmoplasia is increased after sorafenib treatment. This indicates a potential role of hypoxia-induced tumor fibrosis during development of resistance to sorafenib treatment in HCC.

PDGF-B is a profibrotic growth factor whose signaling is blocked by sorafenib.[5,40,41] However, the conversion of HSCs to myofibroblasts during hepatic fibrogenesis or activation of fibroblasts during development of desmoplasia in malignant tumors (e.g., breast cancer) may be directly mediated by other profibrotic and -inflammatory factors, such as SDF-1α.[42-47] Here, we demonstrate, in mouse models of HCC, that increased tumor-associated fibrosis is the result of

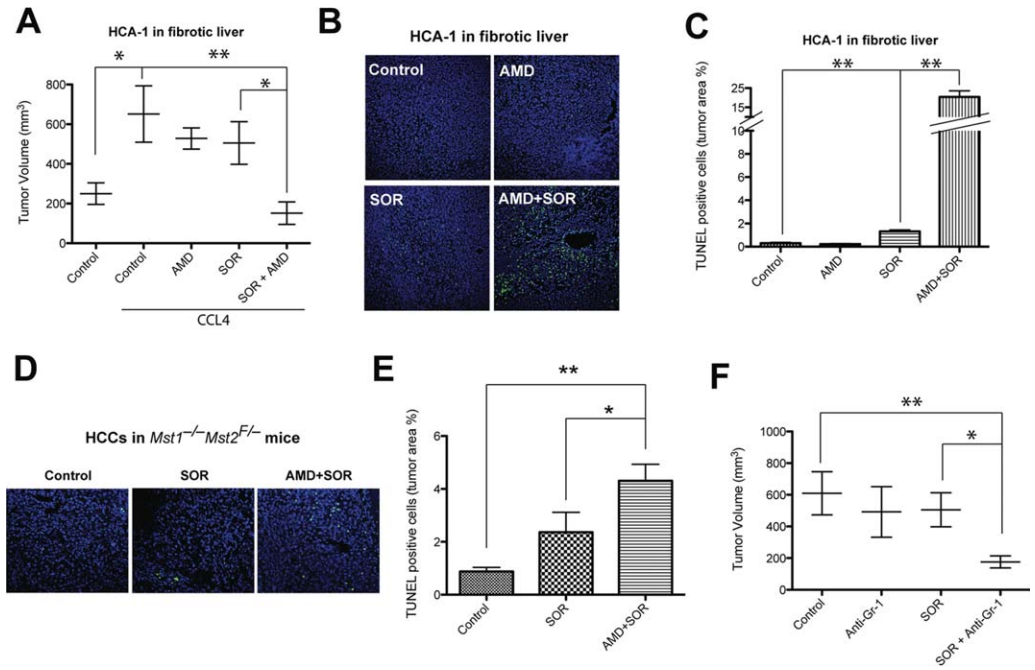

Fig. 7. Sorafenib induces a modest growth delay in HCC, and CXCR4 inhibition or blockade of Gr-1 synergize with sorafenib treatment by increasing cell apoptosis. (A) Sorafenib (SOR) treatment induces a minor, but significant, delay in orthotopic HCC models after 14 days of treatment. HCA-1 tumor growth was delayed by sorafenib in syngeneic C3H mice with underlying liver fibrosis (N = 6-14 mice per group). Whereas treatment with the CXCR4 inhibitor, AMD3100 (AMD), had no effect as monotherapy, AMD3100 with sorafenib induces a more significant tumor growth delay. (B) Representative images of immunofluorescence TUNEL in HCA-1 tumors. Images are 636 μm across. (C) Cell apoptosis, measured by TUNEL, increased after sorafenib treatment in HCA-1 tumors (N = 6-11). (D) Representative images of immunofluorescence of TUNEL in spontaneous HCCs. Images are 636 μm across. (E) Cell apoptosis, measured by TUNEL, increased after sorafenib treatment in spontaneously arising HCCs in $Mst1^{-/-}Mst2^{F/-}$ transgenic mice (N = 6-11). Cell apoptosis was significantly increased when sorafenib treatment was combined with AMD3100 in both tumor models. (F) Combining anti-Gr-1 Abs with sorafenib treatment induced a significant tumor growth delay of orthotopic HCA-1 tumors growing in mice with liver fibrosis (N = 7-13 mice per group). Data are presented as mean ± standard error of the mean. $*P < 0.05$; $**P < 0.01$. TUNEL, terminal deoxynucleotidyl transferase dUTP nick end labeling.

increased myofibroblast infiltration and differentiation mediated by the SDF-1α/CXCR4 pathway (Fig. 8). Our data show that SDF-1α can directly induce HSC differentiation and proliferation through MAPK activation after sorafenib treatment. We also show that SDF1-α can counteract the antifibrotic effects of sorafenib through PDGFR-inhibition—thus leading to increased tumor-associated fibrosis. This led us to test whether CXCR4 blockade could prevent the increase in fibrosis in HCC after sorafenib treatment. Indeed, addition of CXCR4 to sorafenib treatment prevented the increase in tumor-associated fibrosis in the face of persistent hypoxia. Moreover, this combination therapy significantly inhibited HCC growth, compared to sorafenib alone.

Increased SDF-1α expression can also lead to accumulation of tumor-promoting (proangiogenic and immune-suppressive) inflammatory cells.[18,25,48,49] We previously demonstrated that CXCR4 is critical for myeloid cell infiltration in tumors and can compensate for VEGFR1 inhibition in bone-marrow–derived cells by inhibiting CXCR4 with pharmacologic agents and in genetic models.[28] Indeed, we detected an increased infiltration in $Gr\text{-}1^+$ myeloid cells in HCC after sorafenib treatment. Paracrine interactions between stellate cells and inflammatory cells leading to liver fibrosis are also critical in viral hepatitis and pancreatic malignancies.[43-45,50] Here, we demonstrate that $Gr\text{-}1^+$ myeloid cells from sorafenib-treated tumors showed higher expression of multiple profibrotic factors, including SDF-1α and CXCR4, compared to $Gr\text{-}1^+$ myeloid cells from control-treated tumors. Furthermore, we show $Gr\text{-}1^+$ cells directly stimulated the differentiation of HSCs and that the CXCR4 blockade prevented upregulation of collagen I and α-SMA expression in HSCs cocultured with tumor-derived $Gr\text{-}1^+$ myeloid cells. It indicates that the SDF-1α/CXCR4 axis plays an important role mediating not only $Gr\text{-}1^+$ myeloid cell infiltration in HCC, but also their paracrine interaction with HSCs leading to fibrosis. Finally, Ab blockade of Gr-1 reduced $Gr\text{-}1^+$ myeloid cell infiltration, tumor desmoplasia, and HCC growth.

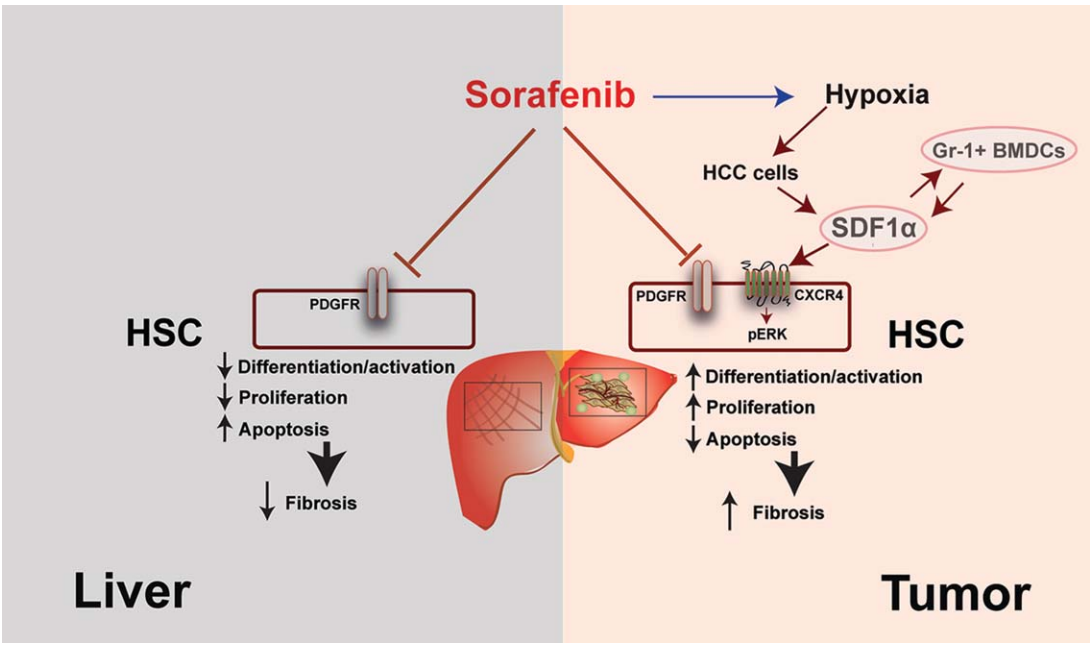

Fig. 8. Differential effect of sorafenib on liver versus tumor-associated fibrosis mediated by the SDF-1α/CXCR4 axis and Gr-1^+ cells in HCC. Differential effects of sorafenib are the result of increased intratumoral hypoxia, leading to elevated SDF-1α expression and Gr-1^+ myeloid cell infiltration. Blocking CXCR4 prevents Gr-1^+ myeloid cell infiltration and HSC differentiation and activation, and synergizes with the antitumor effects of sorafenib.

In conclusion, targeting the SDF-1α/CXCR4 pathway or Gr-1^+ myeloid cell infiltration may be an effective approach to block hypoxia-induced HCC desmoplasia and overcome resistance to sorafenib therapy in HCC.

Acknowledgment: The authors thank D. Nguyen and C. Smith for their outstanding technical support, Drs. J.A. Engelman and C.H. Benes (Massachusetts General Hospital) for their useful discussions, and Dr. Bardeesy for providing the *Mst1*$^{-/-}$*Mst2*$^{F/-}$ transgenic mice.

References

1. Hernandez-Gea V, Toffanin S, Friedman SL, Llovet JM. Role of the microenvironment in the pathogenesis and treatment of hepatocellular carcinoma. Gastroenterology 2013;144:512-527.
2. Hui CK, Leung N, Shek TW, Yao H, Lee WK, Lai JY, et al. Sustained disease remission after spontaneous HBeAg seroconversion is associated with reduction in fibrosis progression in chronic hepatitis B Chinese patients. HEPATOLOGY 2007;46:690-698.
3. Luedde T, Schwabe RF. NF-kappaB in the liver—linking injury, fibrosis and hepatocellular carcinoma. Nat Rev Gastroenterol Hepatol 2011; 8:108-118.
4. Friedman SL. Evolving challenges in hepatic fibrosis. Nat Rev Gastroenterol Hepatol 2010;7:425-436.
5. Wilhelm SM, Carter C, Tang L, Wilkie D, McNabola A, Rong H, et al. BAY 43-9006 exhibits broad spectrum oral antitumor activity and targets the RAF/MEK/ERK pathway and receptor tyrosine kinases involved in tumor progression and angiogenesis. Cancer Res 2004;64: 7099-7109.
6. Almhanna K, Philip PA. Safety and efficacy of sorafenib in the treatment of hepatocellular carcinoma. Onco Targets Ther 2009;2:261-267.
7. Bruix J, Boix L, Sala M, Llovet JM. Focus on hepatocellular carcinoma. Cancer Cell 2004;5:215-219.
8. Cheng AL, Kang YK, Chen Z, Tsao CJ, Qin S, Kim JS, et al. Efficacy and safety of sorafenib in patients in the Asia-Pacific region with advanced hepatocellular carcinoma: a phase III randomised, double-blind, placebo-controlled trial. Lancet Oncol 2009;10:25-34.
9. Llovet JM, Ricci S, Mazzaferro V, Hilgard P, Gane E, Blanc JF, et al. Sorafenib in advanced hepatocellular carcinoma. N Engl J Med 2008; 359:378-390.
10. Zhu AX, Duda DG, Sahani DV, Jain RK. HCC and angiogenesis: possible targets and future directions. Nat Rev Clin Oncol 2011;8: 292-301.
11. Cheng A, Kang Y, Lin D, Park J, Kudo M, Qin S, et al. Phase III trial of sunitinib versus sorafenib in advanced hepatocellular carcinoma. J Clin Oncol 2011;29(Suppl.):abstract 4000.
12. Eckel F, von Delius S, Mayr M, Dobritz M, Fend F, Hosius C, et al. Pharmacokinetic and clinical phase II trial of imatinib in patients with impaired liver function and advanced hepatocellular carcinoma. Oncology 2005;69:363-371.
13. Kaseb AO, Hanbali A, Cotant M, Hassan MM, Wollner I, Philip PA. Vascular endothelial growth factor in the management of hepatocellular carcinoma: a review of literature. Cancer 2009;115:4895-4906.
14. Loges S, Mazzone M, Hohensinner P, Carmeliet P. Silencing or fueling metastasis with VEGF inhibitors: antiangiogenesis revisited. Cancer Cell 2009;15:167-170.
15. Sennino B, McDonald DM. Controlling escape from angiogenesis inhibitors. Nat Rev Cancer 2012;12:699-709.
16. Carmeliet P, Jain RK. Molecular mechanisms and clinical applications of angiogenesis. Nature 2011;473:298-307.
17. Jain RK. Normalizing tumor microenvironment to treat cancer: bench to bedside to biomarkers. J Clin Oncol 2013;31:2205-2218.
18. Duda DG, Kozin SV, Kirkpatrick ND, Xu L, Fukumura D, Jain RK. CXCL12 (SDF1alpha)-CXCR4/CXCR7 pathway inhibition: an emerging sensitizer for anticancer therapies? Clin Cancer Res 2011;17:2074-2080.

19. Farazi PA, DePinho RA. Hepatocellular carcinoma pathogenesis: from genes to environment. Nat Rev Cancer 2006;6:674-687.
20. Friand V, Haddad O, Papy-Garcia D, Hlawaty H, Vassy R, Hamma-Kourbali Y, et al. Glycosaminoglycan mimetics inhibit SDF-1/CXCL12-mediated migration and invasion of human hepatoma cells. Glycobiology 2009;19:1511-1524.
21. Schimanski CC, Bahre R, Gockel I, Muller A, Frerichs K, Horner V, et al. Dissemination of hepatocellular carcinoma is mediated via chemokine receptor CXCR4. Br J Cancer 2006;95:210-217.
22. Xiang ZL, Zeng ZC, Tang ZY, Fan J, Zhuang PY, Liang Y, et al. Chemokine receptor CXCR4 expression in hepatocellular carcinoma patients increases the risk of bone metastases and poor survival. BMC Cancer 2009;9:176.
23. Zhu AX, Sahani DV, Duda DG, di Tomaso E, Ancukiewicz M, Catalano OA, et al. Efficacy, safety, and potential biomarkers of sunitinib monotherapy in advanced hepatocellular carcinoma: a phase II study. J Clin Oncol 2009;27:3027-3035.
24. Zhu AX, Ancukiewicz M, Supko JG, Sahani DV, Blaszkowsky LS, Meyerhardt JA, et al. Efficacy, safety, pharmacokinetics, and biomarkers of cediranib monotherapy in advanced hepatocellular carcinoma: a phase II study. Clin Cancer Res 2013;19:1557-1566.
25. Du R, Lu KV, Petritsch C, Liu P, Ganss R, Passegue E, et al. HIF1alpha induces the recruitment of bone marrow-derived vascular modulatory cells to regulate tumor angiogenesis and invasion. Cancer Cell 2008;13:206-220.
26. Littlepage LE, Egeblad M, Werb Z. Coevolution of cancer and stromal cellular responses. Cancer Cell 2005;7:499-500.
27. Sutton A, Friand V, Brule-Donneger S, Chaigneau T, Ziol M, Sainte-Catherine O, et al. Stromal cell-derived factor-1/chemokine (C-X-C motif) ligand 12 stimulates human hepatoma cell growth, migration, and invasion. Mol Cancer Res 2007;5:21-33.
28. Hiratsuka S, Duda DG, Huang Y, Goel S, Sugiyama T, Nagasawa T, et al. C-X-C receptor type 4 promotes metastasis by activating p38 mitogen-activated protein kinase in myeloid differentiation antigen (Gr-1)-positive cells. Proc Natl Acad Sci U S A 2011;108:302-307.
29. Shojaei F, Wu X, Malik AK, Zhong C, Baldwin ME, Schanz S, et al. Tumor refractoriness to anti-VEGF treatment is mediated by CD11b+Gr1+ myeloid cells. Nat Biotechnol 2007;25:911-920.
30. Zhu AX, Duda DG, Ancukiewicz M, di Tomaso E, Clark JW, Miksad R, et al. Exploratory analysis of early toxicity of sunitinib in advanced hepatocellular carcinoma patients: kinetics and potential biomarker value. Clin Cancer Res 2011;17:918-927.
31. Tofilon PJ, Basic I, Milas L. Prediction of in vivo tumor response to chemotherapeutic agents by the in vitro sister chromatid exchange assay. Cancer Res 1985;45:2025-2030.
32. Das A, Shergill U, Thakur L, Sinha S, Urrutia R, Mukhopadhyay D, Shah VH. Ephrin B2/EphB4 pathway in hepatic stellate cells stimulates Erk-dependent VEGF production and sinusoidal endothelial cell recruitment. Am J Physiol Gastrointest Liver Physiol 2010;298:G908-G915.
33. Kim W, Seong J, Oh HJ, Koom WS, Choi KJ, Yun CO. A novel combination treatment of armed oncolytic adenovirus expressing IL-12 and GM-CSF with radiotherapy in murine hepatocarcinoma. J Radiat Res 2011;52:646-654.
34. Zhou D, Conrad C, Xia F, Park JS, Payer B, Yin Y, et al. Mst1 and Mst2 maintain hepatocyte quiescence and suppress hepatocellular carcinoma development through inactivation of the Yap1 oncogene. Cancer Cell 2009;16:425-438.
35. Kim SU, Oh HJ, Wanless IR, Lee S, Han KH, Park YN. The Laennec staging system for histological sub-classification of cirrhosis is useful for stratification of prognosis in patients with liver cirrhosis. J Hepatol 2012;57:556-563.
36. Huang Y, Yuan J, Righi E, Kamoun WS, Ancukiewicz M, Nezivar J, et al. Vascular normalizing doses of antiangiogenic treatment reprogram the immunosuppressive tumor microenvironment and enhance immunotherapy. Proc Natl Acad Sci U S A 2012;109:17561-17566.
37. Bai Q, An J, Wu X, You H, Ma H, Liu T, et al. HBV promotes the proliferation of hepatic stellate cells via the PDGF-B/PDGFR-beta signaling pathway in vitro. Int J Mol Med 2012;30:1443-1450.
38. Liu Y, Lui EL, Friedman SL, Li L, Ye T, Chen Y, et al. PTK787/ZK22258 attenuates stellate cell activation and hepatic fibrosis in vivo by inhibiting VEGF signaling. Lab Invest 2009;89:209-221.
39. Wang Y, Gao J, Zhang D, Zhang J, Ma J, Jiang H. New insights into the antifibrotic effects of sorafenib on hepatic stellate cells and liver fibrosis. J Hepatol 2010;53:132-144.
40. Pinzani M, Milani S, Herbst H, DeFranco R, Grappone C, Gentilini A, et al. Expression of platelet-derived growth factor and its receptors in normal human liver and during active hepatic fibrogenesis. Am J Pathol 1996;148:785-800.
41. Lederle W, Stark HJ, Skobe M, Fusenig NE, Mueller MM. Platelet-derived growth factor-BB controls epithelial tumor phenotype by differential growth factor regulation in stromal cells. Am J Pathol 2006;169:1767-1783.
42. Kojima Y, Acar A, Eaton EN, Mellody KT, Scheel C, Ben-Porath I, et al. Autocrine TGF-beta and stromal cell-derived factor-1 (SDF-1) signaling drives the evolution of tumor-promoting mammary stromal myofibroblasts. Proc Natl Acad Sci U S A 2010;107:20009-20014.
43. Mitra P, Shibuta K, Mathai J, Shimoda K, Banner BF, Mori M, Barnard GF. CXCR4 mRNA expression in colon, esophageal and gastric cancers and hepatitis C infected liver. Int J Oncol 1999;14:917-925.
44. Terada R, Yamamoto K, Hakoda T, Shimada N, Okano N, Baba N, et al. Stromal cell-derived factor-1 from biliary epithelial cells recruits CXCR4-positive cells: implications for inflammatory liver diseases. Lab Invest 2003;83:665-672.
45. Wald O, Pappo O, Safadi R, Dagan-Berger M, Beider K, Wald H, et al. Involvement of the CXCL12/CXCR4 pathway in the advanced liver disease that is associated with hepatitis C virus or hepatitis B virus. Eur J Immunol 2004;34:1164-1174.
46. Hong F, Tuyama A, Lee TF, Loke J, Agarwal R, Cheng X, et al. Hepatic stellate cells express functional CXCR4: role in stromal cell-derived factor-1alpha-mediated stellate cell activation. HEPATOLOGY 2009;49:2055-2067.
47. Sawitza I, Kordes C, Reister S, Haussinger D. The niche of stellate cells within rat liver. HEPATOLOGY 2009;50:1617-1624.
48. Facciabene A, Peng X, Hagemann IS, Balint K, Barchetti A, Wang LP, et al. Tumour hypoxia promotes tolerance and angiogenesis via CCL28 and T(reg) cells. Nature 2011;475:226-230.
49. Hanahan D, Coussens LM. Accessories to the crime: functions of cells recruited to the tumor microenvironment. Cancer Cell 2012;21:309-322.
50. Beatty GL, Chiorean EG, Fishman MP, Saboury B, Teitelbaum UR, Sun W, et al. CD40 agonists alter tumor stroma and show efficacy against pancreatic carcinoma in mice and humans. Science 2011;331:1612-1616.